

# Seismic fragility assessment of optimally designed steel moment frames

Fayegh Fattahi, Saeed Gholizadeh\*

Department of Civil Engineering, Urmia University, Urmia, Iran



## ARTICLE INFO

### Keywords:

Performance-based design  
Optimization  
Incremental dynamic analysis  
Collapse-resistance capacity  
Fragility assessment  
Steel moment frame

## ABSTRACT

This study is devoted to seismic performance assessment of optimally designed steel moment frames (SMFs) in the framework of performance-based design (PBD). The methodology presented in this work includes three phases. The first phase involves the optimization of SMFs by employing an efficient metaheuristic algorithm to meet the PBD requirements according to FEMA-350 code. Subsequently, the overall damage index (*ODI*) is calculated for the obtained optimal SMFs based on the Park-Ang local damage index ( $DI_{PA}$ ). In the second phase, incremental dynamic analysis (IDA) is conducted for the optimally designed SMFs and their fragility curves are derived and their collapse margin ratios (*CMRs*) are determined based on FEMA-P695. In the last phase, the fragility curves of the optimal SMFs are generated for different damage levels ranging from slight damage to collapse state and a new damage measure termed as damage margin ratio (*DMR*) is introduced to assess the damage-resistance capacity of the SMFs at the different damage levels. In order to illustrate the efficiency of the proposed methodology, three numerical examples of 3-, 6-, and 12-story SMFs are presented and the total cost of optimal SMFs, including initial and seismic damage costs, are determined. The numerical results demonstrate that the SMF with the best total cost has the best *CMR*, *DMR*, and degree of reparability.

## 1. Introduction

In the last years, performance-based design (PBD) has emerged as one of the most efficient seismic design approaches which its main purpose is to design structures that present a predictable and reliable behavior against seismic actions through their lifespan. It is expected that the structures designed according to the PBD methodologies will resist earthquakes by tolerating levels of seismic damage. The structures designed in the framework of PBD satisfy a sort of predefined performance levels about their corresponding hazard levels. An efficient design framework may be offered by integrating PBD methodologies and structural optimization techniques. During the last few years some researches have been conducted in this context for steel structures. Choi and Park [1] employed a non-dominated sorting genetic algorithm-II (NSGA-II) for seismic PBD optimization of SMFs to ensure beam-hinging mechanism. Saadat et al. [2] achieved multi-objective PBD optimization of a SMF taking into account two conflicting objective functions: direct social and economic losses. Gholizadeh [3] utilized a combination of neural network (NN) and a modified firefly algorithm (MFA) for PBD optimization of SMFs. Gholizadeh and Poorhoseini [4] proposed a methodology for optimal placement of braces in steel braced frames (SBF) in the framework of PBD using an improved dolphin echolocation algorithm. Xu et al. [5] employed generalized pattern search (GPS)

algorithm to implement multi-objective PBD optimization of steel frames subject to random excitation. Gholizadeh and Baghchevan [6] proposed a chaotic multi-objective firefly algorithm (CMOFA) for finding the Pareto front of the multi-objective PBD optimization problem of SMFs.

The last decades have witnessed a great effort to develop procedures for seismic assessment of structures because, the most important issue that the engineers and designers have to deal with is to evaluate the collapse safety of the structures. In order to achieve this purpose, the fragility assessment of structures can be carried out to provide a measure of the safety margin for the structures. The collapse fragility curves are often developed to characterize the fragility of structures subject to earthquake. A simplified methodology was proposed by Shafei et al. [7] to predict the collapse capacity of SMF and shear wall structural systems. They employed a database of collapse fragilities and pushover curves to develop closed-form equations. Hardyniec and Charney [8] proposed a parallel computing-based methodology to determine the collapse margin ratio (*CMR*) of steel structures which does not require the implementation of incremental dynamic analysis (IDA) [9]. Asgarian and Ordoubadi [10] studied effects of inherent uncertainties on seismic performance of SMFs through seismic fragility analysis of ordinary and special SMFs for different performance limit states. Cha and Bai [11] achieved seismic fragility assessment of a SMF controlled by

\* Corresponding author at: Department of Civil Engineering, Urmia University, P.O. box 165, Urmia, Iran.

E-mail address: [s.gholizadeh@urmia.ac.ir](mailto:s.gholizadeh@urmia.ac.ir) (S. Gholizadeh).

magnetorheological dampers with a direct PBD procedure by developing fragility curves considering four capacity limits.

Today, literature on the fragility assessment of optimally designed structures is so sparse and there is a serious lack of information in this regard. In fact, this is the first paper to evaluate the seismic collapse safety of SMF structures optimized in the framework of PBD. In order to carry out the PBD optimization task of SMFs an efficient and robust optimization algorithm should be utilized to minimize an objective function subject to several constraints on performance capabilities. In the present work, enhanced colliding bodies optimization-II (ECBO-II) [12] is selected as the optimizer to find optimal solutions for PBD optimization problem of SMF structures. ECBO-II is a modified version of the ECBO [13] metaheuristic which is based on the collision phenomenon between two bodies in which the velocity and position of the bodies are updated in a way that their energy level reaches a minimum value. The merit of ECBO-II over a sort of metaheuristics has been demonstrated in [12] for tackling the PBD optimization problem of SMFs. In order to account for the stochastic nature of the ECBO-II metaheuristic algorithm, twenty-five independent PBD optimization runs are carried out for SMFs based on FEMA-350 [14] provisions. In the next stage, collapse capacity of the best five optimal structures is evaluated based on FEMA-P695 [15] methodology. For this purpose, IDA curves need to be determined by conducting a number of nonlinear response-history analyses for a suite of records scaled at increasing intensity levels. Then, the collapse safety of the optimal designs is determined by the fragility assessment that can be achieved based on the IDA results at collapse. One of the most important issues in performing incremental dynamic analyses is selecting an appropriate damage measure. Maximum inter-story drift ratio is the most commonly used damage measure in the framework of IDA.

In order to quantify the level of damage in structures subject to earthquake, a more accurate damage index (DI) should be taken into account. During the last decades several DIs have been developed and one of the popular ones is the so-called Park-Ang [16] damage index ( $DI_{PA}$ ) which combines the ductility and cumulative energy demands. The  $DI_{PA}$  is locally defined for structural elements however, an overall damage index (ODI) may be defined for whole the structure to compute its seismic damage cost. The seismic damage cost can then be added to the structural initial cost to characterize the life cycle or total cost of the structure. In the present study, in order to assess the performance of SMFs, not only in collapse point but also in different levels of damage, ODI-based fragility curves are derived for various damage levels and a new damage measure named as damage margin ratio (DMR) is defined for the optimal designs. The mean value of ODIs at collapse is then used to determine the reparability border of the SMFs and to compute the seismic damage cost and consequently the total cost of the structures. The effectiveness of the proposed methodology is illustrated through three numerical examples of 3-, 6-, and 12-story SMF structures. The numerical results reveal that the structures with the best overall cost have the best distribution of local damages which leads to the highest CMR and DMR values. This observation clearly supports the importance of optimization of structural total cost in order to design safe and cost-efficient structures subject to earthquake.

## 2. Performance-based design optimization

PBD is a modern methodology for the seismic design of structures to increase the safety of structures in their lifespan in which performance is divided into some levels each corresponding to a hazard level. In the framework of PBD, structural nonlinear response needs to be evaluated at predefined performance levels to identify the seismic damage levels. In other words, PBD attempts to evaluate structures at different damage states under specific levels of seismic hazards. In this work, immediate occupancy (IO) and collapse prevention (CP) are considered as the performance levels. Moreover, maximum considered earthquake (MCE) and frequent earthquake (FE) ground motions respectively, with less

than 2% and 50% probability of exceedance in 50 years are taken into account as two hazard levels based on FEMA-350 [14], named here as 2/50 and 50/50 hazard levels. On the other hand, the number of parameters affecting the seismic performance of structures is so large which makes it difficult to recognize that the current solution is the optimum design or still there is room for improving the design. In order to design cost-efficient structures having appropriate seismic performance, structural optimization techniques can be effectively utilized.

In the PBD optimization process of SMFs proposed in the present study, structural weight is treated as the objective function (OF), while the seismic performance requirements, in accordance with FEMA-350, are treated as the PBD constraints. In this case, the constraints for confidence level (CL) for CP and IO performance levels are considered as follows:

$$1 \leq \frac{CL_{IO}}{CL'_{IO}} \quad (1)$$

$$1 \leq \frac{CL_{CP}}{CL'_{CP}} \quad (2)$$

where  $CL'_{IO}$  and  $CL'_{CP}$  are considered confidence levels of IO and CP performance levels, respectively which both are chosen to be 90% in the present study.

In the performance evaluation process, inter-story drifts (structural response parameters) are determined for suites of earthquakes in 2/50 and 50/50 hazard levels using nonlinear response-history analysis. To determine the CL for each hazard level, the factored-demand-to-capacity ratio ( $\lambda$ ) is computed as

$$\lambda = \frac{\gamma \gamma_a D}{\phi C} \quad (3)$$

where  $\gamma$  and  $\gamma_a$  are a demand variability factor and an analysis uncertainty factor, respectively;  $D$  and  $C$  are the calculated demand and the capacity of the structure, respectively; and  $\phi$  is a resistance factor for considering the uncertainty and variability in the prediction of structural capacity [14].

To compute the CL for each hazard level the following equation is used:

$$CL = \Phi \left( \frac{k\beta_{UT}}{2} - \frac{\ln(\lambda)}{b\beta_{UT}} \right) \quad (4)$$

where  $\Phi$  is the normal cumulative distribution function;  $k$  is the slope of the hazard curve, in ln- coordinates, at the hazard level of interest;  $\beta_{UT}$  is an uncertainty measure equal to the vector sum of the logarithmic standard deviation of the variations in demand and capacity resulting from uncertainty; and  $b = 1.0$  [14].

Furthermore, serviceability and strong column/weak beam (SCWB) requirements have to be considered in the optimization process, respectively based on AISC 360-16 [17] and AISC 341-16 [18] design codes. As the serviceability constraints strength of beams and columns of SMFs is checked for only gravity loads and geometry of the beam-column connections is checked to ensure constructability of the structures [19]. Moreover, the SCWB constraint is checked to prevent the formation of weak or soft story mechanisms.

The formulation of the PBD optimization problem of SMFs with  $n_g$  design variable groups and  $n_c$  design constraints is presented as follows:

$$\text{Find: } X = \{x_1, x_2, \dots, x_{n_g}\}^T \quad (5)$$

$$\text{To minimize: } OF(X) \quad (6)$$

$$\text{Subject to: } g_i(X) \leq 0, \quad i = 1, 2, \dots, n_c \quad (7)$$

where  $X$  is a vector of design variables;  $OF$  is the objective function to be minimized; and  $g_i$  is the  $i$ th design constraint.

In this study, in order to solve the formulated optimization problem, an efficient metaheuristic algorithm, i.e. enhanced colliding bodies

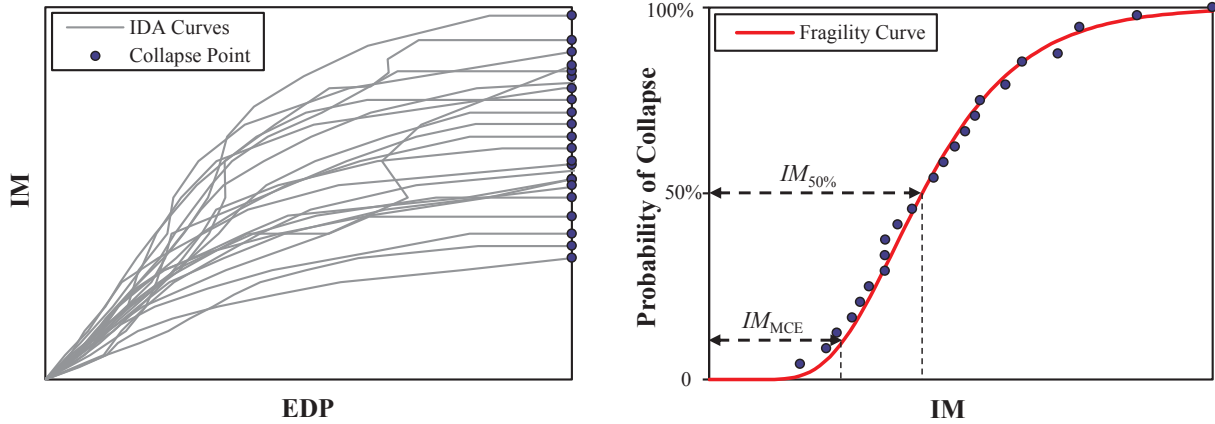


Fig. 1. Schematic of the typical IDA curves and fragility curve generation using the collapse data.

optimization-II (ECBO-II) [12], is utilized which its computational merit in tackling the problem of PBD optimization of steel SMF structures has been demonstrated in [12].

### 3. Seismic damage indices

The assessment of the severity of local damage in structural members and overall damage in the structure during earthquake is usually achieved by the means of a damage index (DI). One of the most frequently employed DIs is the so-called Park-Ang DI ( $DI_{PA}$ ) [15] which its efficiency in representing the actual state of damage in steel structures has been demonstrated in literature [20]. The use of the  $DI_{PA}$  as a better alternative to the inter-story drift (or residual drift) is not always justified. In fact, quite a few studies [21,22] have revealed that hysteretic energy dissipation is not consistently in good correlation with seismic performance. Hence, the selection of an energy-based DI could render the comparison of structural systems with different hysteretic characteristics (e.g. different connection typologies) problematic. In the present work, it is assumed that the considered SMF structures have the same connection typology. For the structural members, local  $DI_{PA}$  is defined as follows [20]:

$$DI_{PA} = \frac{\theta_m - \theta_r}{\theta_u - \theta_r} + \frac{\beta}{\theta_u M_y} \int dE \quad (8)$$

where  $\theta_m$  and  $\theta_u$  is the maximum rotation of the structural element end-section and its ultimate rotation capacity, respectively;  $\theta_r$  represents the recoverable rotation during unloading;  $\beta$  is a strength deteriorating constant; and  $M_y$  is the yield moment of the structural element.

The damage indices are classified as local and global DIs based on their application for quantifying of damage in individual members or entire building, respectively. It is obvious that the overall damage of a structure is a function of its members' damages and their distribution throughout the structure. As the damage distribution is closely related to the distribution of the absorbed energy, the overall damage index (ODI) of a structure can be represented by a weighted summation of members' local DIs as follows [23]:

$$ODI = \sum_{i=1}^{ne} \alpha_i \cdot DI_{PA,i} \quad (9)$$

$$\alpha_i = E_i / \sum_{i=1}^{ne} E_i \quad (10)$$

where  $ne$  is the number of elements;  $E_i$  is the absorbed hysteretic energy by the  $i$ th member.

As the  $ODI$  is an indicator of structural distress, the seismic repair cost of a structure can be calculated based on this index as  $C_R(ODI)$  occurring at a time  $t$ . A common form of  $C_R(ODI)$  may be expressed as

follows [24]:

$$C_R(ODI) = \eta \cdot C_0 \cdot \left( \frac{ODI}{ODI_R} \right) \quad (11)$$

where  $\eta$  is a factor to account for demolition and clearing and in the present work is considered to be 1.5;  $ODI_R$  is a reparability overall damage index which is usually taken as 0.6 for RC structures [24] and in the present paper, its values are computed for steel structures based on the results of IDA;  $C_0$  is the complete replacement cost of SMF which here is taken as its structural weight as follows:

$$C_0 = \sum_{i=1}^{ne} \rho_i \cdot A_i \cdot L_i \quad (12)$$

where  $\rho_i$ ,  $A_i$  and  $L_i$  are the weight density, cross-sectional area and length of the  $i$ th structural member, respectively.

The deterministic expected present repair cost,  $C_{RE}$ , is computed as follows [24]:

$$C_{RE} = \int_0^{\infty} v C_R(ODI) e^{-(r+v)t} dt = \frac{v}{r+v} C_R(ODI) \quad (13)$$

where  $r$  and  $v$  are the discount rate and a Poisson coefficient, respectively which in the present study are taken as  $r = 0.05$  and  $v = 1$ .

As a result, the total cost of the structures ( $C_T$ ) can be simply defined as follows:

$$C_T = C_0 + C_{RE} \quad (14)$$

In this work,  $C_0$  is taken as the objective function of the PBD optimization problem, and the obtained optimal designs are compared in terms of  $C_T$ .

### 4. Collapse margin ratio

Quantification of structural performance based on seismic collapse capacity is one of the reasonable methodologies for seismic evaluation of structural systems. FEMA-P695 proposes an efficient framework based on IDA to assess the collapse safety of structures in which numerous nonlinear response-history analyses need to be conducted for a suit of 22 ground motions scaled to MCE. In fact, IDA is a technique to process the effect of a ground motion intensity measure (IM) on an engineering demand parameter (EDP) up to collapse. The IM and EDP are usually taken as 5% damped spectral acceleration at fundamental period,  $S_a(T_1, 5\%)$ , and maximum inter-story drift ratio,  $d_{max}$ , respectively. In the framework of IDA, a nonlinear response-history analysis of structures subject to increasingly scaled records is implemented and IDA curves are obtained by recording the EDP versus the IM and the process is continued until one of the following collapse criteria is met:

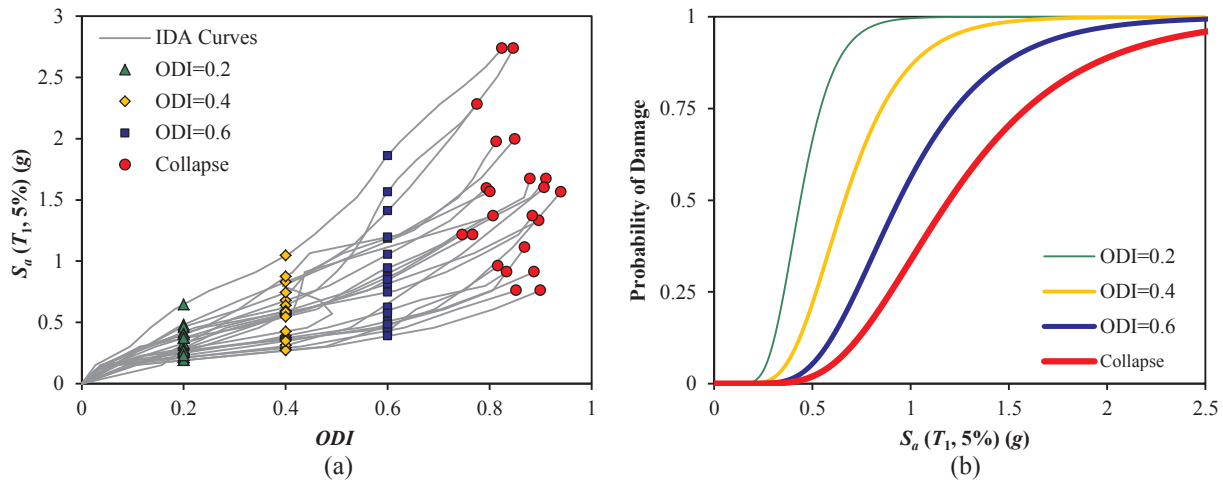


Fig. 2. Schematic of (a) typical ODI-based IDA curves and (b) fragility curves for different damage states.

Table 1  
Damage states based on overall Park-Ang damage index [30].

Damage state	ODI	Comments
Minor	0.0–0.2	Minor damage
Moderate	0.2–0.4	Repairable
Severe	0.4–1.0	Beyond repair
Collapse	1.0 <	Loss of building

Table 2  
Ground motion records set.

No.	Earthquake			Record motion		
	M	Year	Name	Record station	PGA <sub>max</sub> (g)	PGV <sub>max</sub> (cm/s)
1	6.7	1994	Northridge	Beverly Hills - Mulhol Canyon	0.52	63
2	6.7	1994	Northridge	Country-WLC	0.48	45
3	7.1	1999	Duzce, Turkey	Bolu	0.82	62
4	7.1	1999	Hector Mine	Hector	0.34	42
5	6.5	1979	Imperial Valley	Delta	0.35	33
6	6.5	1979	Imperial Valley	El Centro Array #11	0.38	42
7	6.9	1995	Kobe, Japan	Nishi-Akashi	0.51	37
8	6.9	1995	Kobe, Japan	Shin-Osaka	0.24	38
9	7.5	1999	Kocaeli, Turkey	Duzce	0.36	59
10	7.5	1999	Kocaeli, Turkey	Arcelik	0.22	40
11	7.3	1992	Landers	Yermo Fire Station	0.24	52
12	7.3	1992	Landers	Coolwater	0.42	42
13	6.9	1989	Loma Prieta	Capitola	0.53	35
14	6.9	1989	Loma Prieta	Gilroy Array #3	0.56	45
15	7.4	1990	Manjil, Iran	Abbar	0.51	54
16	6.5	1987	Superstition Hills	El Centro Imp. Co.	0.36	46
17	6.5	1987	Superstition Hills	Poe Road (temp)	0.45	36
18	7.0	1992	Cape Mendocino	Rio Dell Overpass	0.55	44
19	7.6	1999	Chi-Chi, Taiwan	CHY101	0.44	115
20	7.6	1999	Chi-Chi, Taiwan	TCU045	0.51	39
21	6.6	1971	San Fernando	LA - Hollywood Stor	0.21	19
22	6.5	1976	Friuli, Italy	Tolmezzo	0.35	31

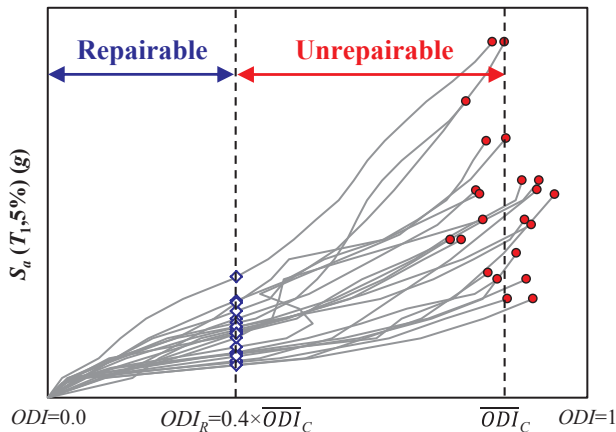


Fig. 3. Repairable and unreparable regions in the  $S_a$ -ODI space.

- Maximum inter-story drift ratio ( $d_{max}$ ) exceeds 0.1
- The slope of the IDA curves decreases to a value less than 0.2 of the median of their initial slope
- The structure collapses due to plastic hinges formation in its members.

As the subsequent step in the collapse safety assessment process, the fragility curve must be generated for the structure at hand using the IM values associated with the collapse state from a set of IDA curves which relates the IM to the probability of collapse by fitting a lognormal distribution function to the collapse data. FEMA-P695 defines the  $CMR$  as the ratio of the spectral acceleration for which half of the pre-defined earthquake records cause collapse (denoted as  $IM_{50\%}$ ) to the spectral acceleration of the MCE ground motion (denoted as  $IM_{MCE}$ ). The schematic of the fragility curve generation based on the collapse data is depicted in Fig. 1.

Accordingly,  $CMR$  can be computed as follows based on FEMA-P695:

$$CMR = \frac{IM_{50\%}}{IM_{MCE}} \tag{15}$$

It is obvious that the larger value of  $CMR$  implies that the structure has a higher level of seismic collapse safety.

Frequency content or spectral shape of a suit of earthquake records set can significantly affect the calculation of  $CMR$  and consequently the seismic collapse safety of a structure. In order to address the spectral shape effects, an adjusted collapse margin ratio ( $ACMR$ ) is defined as follows [15]:

$$ACMR = SSF \times CMR \tag{16}$$

where  $SSF$  is the spectral shape factor which depends on fundamental period and period-based ductility determined from Table 7-1 of FEMA-

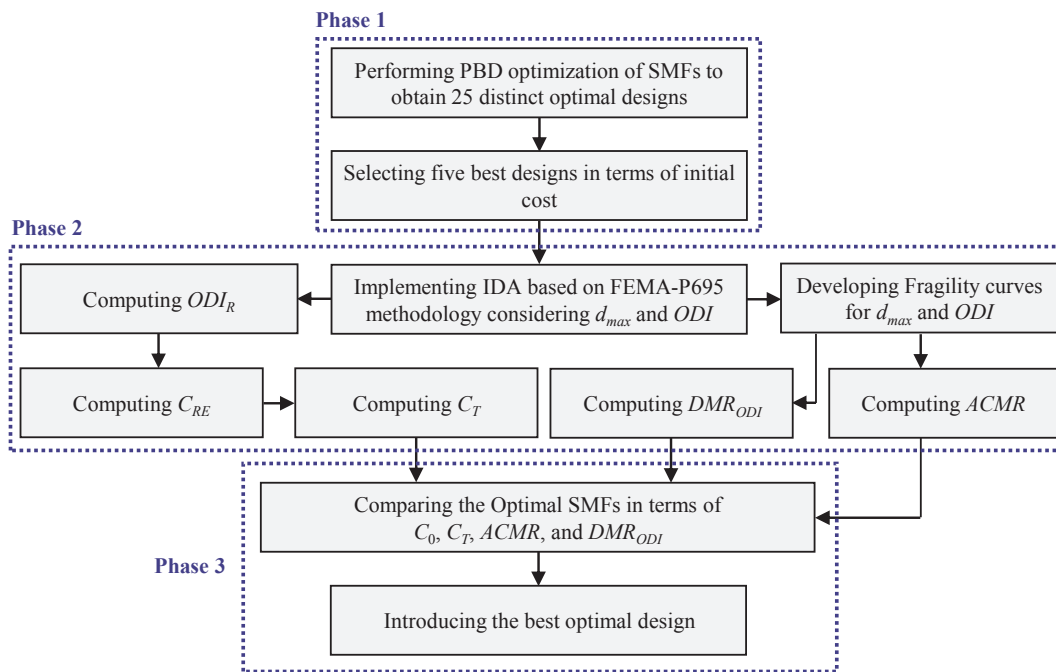


Fig. 4. Flowchart of the proposed methodology.

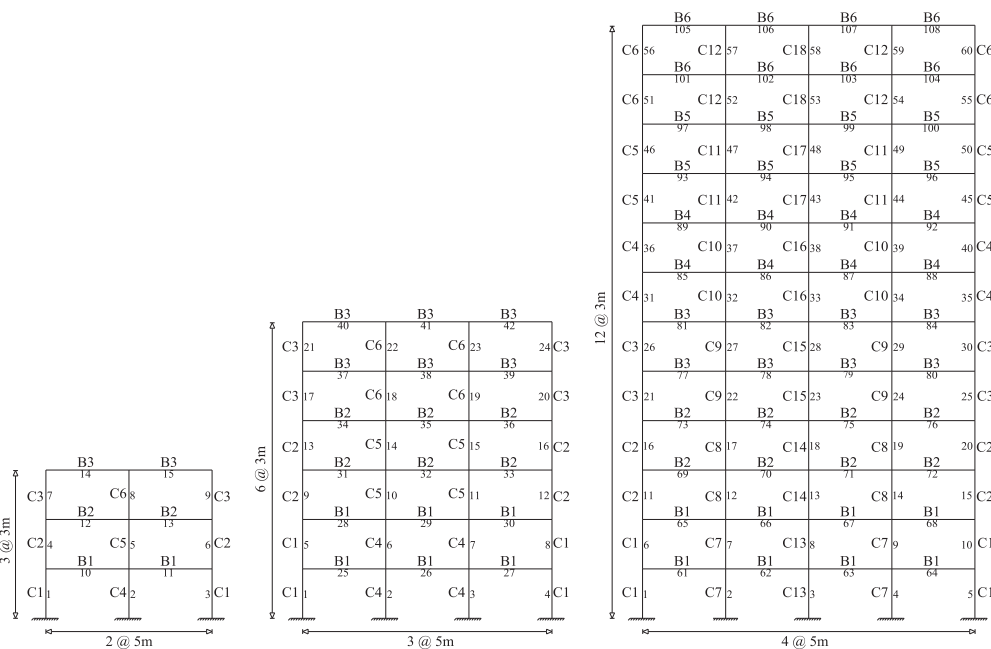


Fig. 5. Topology and grouping details of 3-, 6-, and 12-story SMFs.

Table 3  
List of available sections for columns and beams.

Column			Beam	
W14 × 30	W14 × 82	W14 × 193	W12 × 26	W18 × 46
W14 × 34	W14 × 90	W14 × 211	W12 × 30	W18 × 50
W14 × 38	W14 × 99	W14 × 233	W12 × 35	W18 × 60
W14 × 43	W14 × 109	W14 × 257	W12 × 40	W21 × 44
W14 × 48	W14 × 120	W14 × 283	W16 × 26	W21 × 55
W14 × 53	W14 × 132	W14 × 311	W16 × 36	W21 × 57
W14 × 61	W14 × 145	W14 × 342	W16 × 45	W24 × 55
W14 × 68	W14 × 159	W14 × 370	W16 × 57	W24 × 62
W14 × 74	W14 × 176	W14 × 398	W18 × 35	W24 × 68

P695 [15].

The total system collapse uncertainty,  $\beta_{TOT}$ , is one of the most important factors in evaluation of collapse safety which is calculated by combining uncertainty sources of record-to-record ( $\beta_{RTR}$ ), design requirements ( $\beta_{DR}$ ), test data ( $\beta_{TD}$ ), and modeling ( $\beta_{MDL}$ ) as follows:

$$\beta_{TOT} = \sqrt{\beta_{RTR} + \beta_{DR} + \beta_{TD} + \beta_{MDL}} \tag{17}$$

The shape of collapse fragility curve and consequently the acceptable values of ACMR are highly influenced by  $\beta_{TOT}$ . In the present study, the values of  $\beta_{RTR}$ ,  $\beta_{DR}$ ,  $\beta_{TD}$ , and  $\beta_{MDL}$  are taken as 0.4, 0.1, 0.2, and 0.2, respectively, for which Eq. (17) gives  $\beta_{TOT} = 0.5$ .

**Table 4**  
Five best optimal solutions for 3-story SMF.

Design variables	Optimum performance-based solutions				
	S1	S2	S3	S4	S5
C1	W14 × 34	W14 × 38	W14 × 34	W14 × 38	W14 × 48
C2	W14 × 34	W14 × 38	W14 × 34	W14 × 38	W14 × 48
C3	W14 × 30	W14 × 30	W14 × 30	W14 × 30	W14 × 30
C4	W14 × 68	W14 × 61	W14 × 68	W14 × 68	W14 × 68
C5	W14 × 68	W14 × 61	W14 × 68	W14 × 68	W14 × 68
C6	W14 × 53	W14 × 53	W14 × 43	W14 × 48	W14 × 53
B1	W12 × 30	W12 × 30	W12 × 35	W12 × 30	W12 × 30
B2	W12 × 35	W12 × 35	W12 × 35	W12 × 35	W12 × 30
B3	W12 × 26	W12 × 26	W10 × 26	W10 × 26	W12 × 26
C <sub>0</sub> (kg)	3075.66	3084.75	3104.59	3123.84	3218.36
CL <sub>10</sub> (%)	98.96	98.97	99.40	99.08	98.96
CL <sub>CP</sub> (%)	99.84	99.83	99.93	99.89	99.91

**5. Margin ratio for different levels of damage**

In fact, *CMR* is a measure of the collapse safety and reflects the resistance of structures against collapse without providing any information regarding the damage spreading in the structures. Assessment of performance of structures at various levels of damage and defining a safety margin for structural repairability is of great importance. In most cases, the level of seismic damage in framed structures is characterized using *DIs* based on inter-story drift ratio [25,26] however, these *DIs* do not consider the total energy dissipated by the structural systems during an earthquake and therefore the seismic performance of structures cannot be adequately characterized through these *DIs* [27–29]. On the other hand, the maximum inter-story drift ratio cannot reflect the seismic damage distribution through the structure. In such a case, the overall damage index, defined by Eq. (9), eliminates the mentioned drawbacks of the maximum inter-story drift ratio and therefore it can be utilized as an efficient alternate EDP to conduct IDA.

In this study, *ODI* is taken into account as the EDP and IDA curves are extracted for the structures by recording *ODI* versus *S<sub>a</sub>*(*T*<sub>1</sub>, 5%). The generated *ODI*-based IDA curves can be used to generate fragility curves for various damage levels characterized by *ODI*. A sort of typical *ODI*-based IDA curves and four fragility curves for different damage states are depicted in Fig. 2. An indicator is proposed to assess the performance of structures in each level of damage ranging from *ODI* = 0.0 to *ODI* at collapse. The proposed indicator is termed as damage margin

ratio (*DMR*) and is defined for each level of damage as the ratio of *S<sub>a</sub>* for which half of records give *ODIs* greater than an specific *ODI* to the *S<sub>a</sub>* *MCE*:

$$DMR_{ODI} = \frac{(S_{a50\%})_{ODI}}{S_{aMCE}}, \quad ODI = 0.0, \dots, \text{Collapse} \tag{18}$$

where (*S<sub>a</sub>* 50%)*ODI* denotes the spectral acceleration for which 50% records exceed an specific *ODI*.

A classification for identifying different damage levels of structures based on *ODI* has been developed in ATC-13 [30] given in Table 1.

It can be observed that *ODI* ≤ 0.4 implies that the structure is repairable, 0.4 ≤ *ODI* ≤ 1.0 means damage beyond repair, and total collapse is represented by 1.0 ≤ *ODI* [23,30]. As regards the damage distribution in low-, mid-, and high-rise structures is not the same, it is not rational to consider the same repairability index (i.e. *ODI* = 0.4) for the structures with different heights. Furthermore, our numerical results demonstrate that Eqs. (8)–(10) give an *ODI* less than unity at collapse points of structures and this means that the repairability border of Table 1 (i.e. *ODI* = 0.4) needs to be slightly modified. In the present work, an attempt is done to determine a distinct repairability index for low-, mid-, and high-rise optimally designed SMFs reflecting their distribution of damage. In this way, as shown in Fig. 3, the mean value of *ODI* at collapse, *ODI<sub>C</sub>*, is calculated and the overall damage index representing the repairability border, *ODI<sub>R</sub>*, is taken as 40% of *ODI<sub>C</sub>*.

$$ODI_C = \frac{1}{Nr} \sum_{i=1}^{Nr} ODI_{C,i} \tag{19}$$

$$ODI_R = 0.4 \times ODI_C \tag{20}$$

where *Nr* is the number of records used to conduct IDA, and *ODI<sub>C,i</sub>* is overall damage index at collapse point of *i*th record.

**6. Proposed methodology**

This section describes the methodology proposed in the present work to conduct seismic assessment of optimally designed 3-, 6-, and 12-story SMFs in the framework of PBD. The proposed methodology includes three phases as explained below.

In the first phase, The optimization task is achieved using ECBO-II [12] algorithm as its computational advantages in dealing with PBD optimization problems of SMFs has been already demonstrated in [12]. The objective function of the optimization process is initial cost of the SMFs given by Eq. (12). Herein, ground motion records listed in

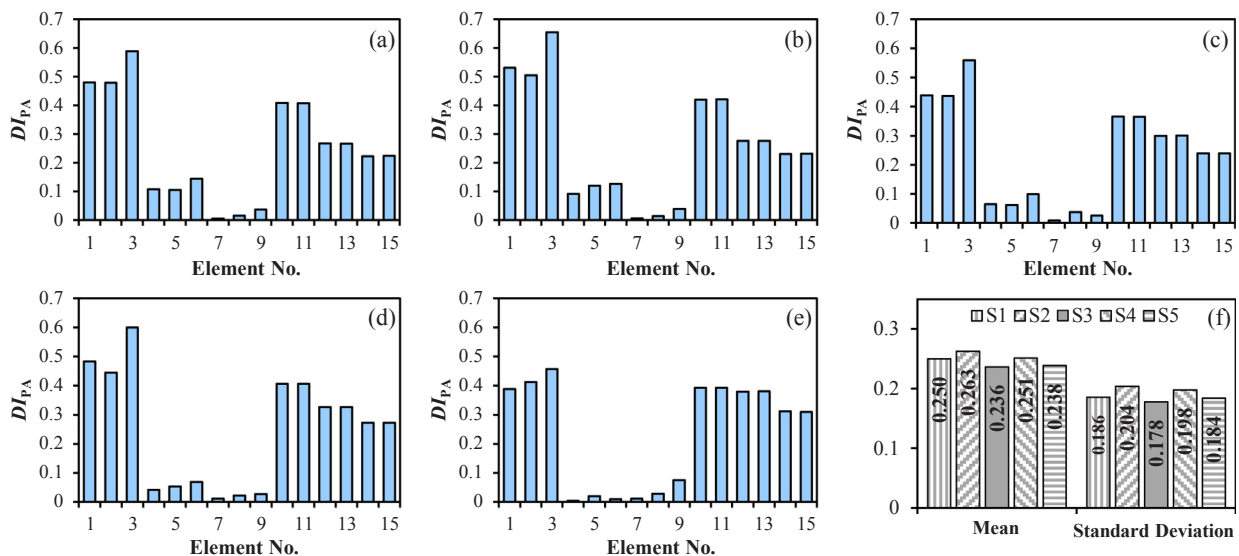


**Fig. 6.** *DI<sub>PA</sub>* for members of 3-story (a) S1, (b) S2, (c) S3, (d) S4, (e) S5, and (f) their mean and standard deviation.

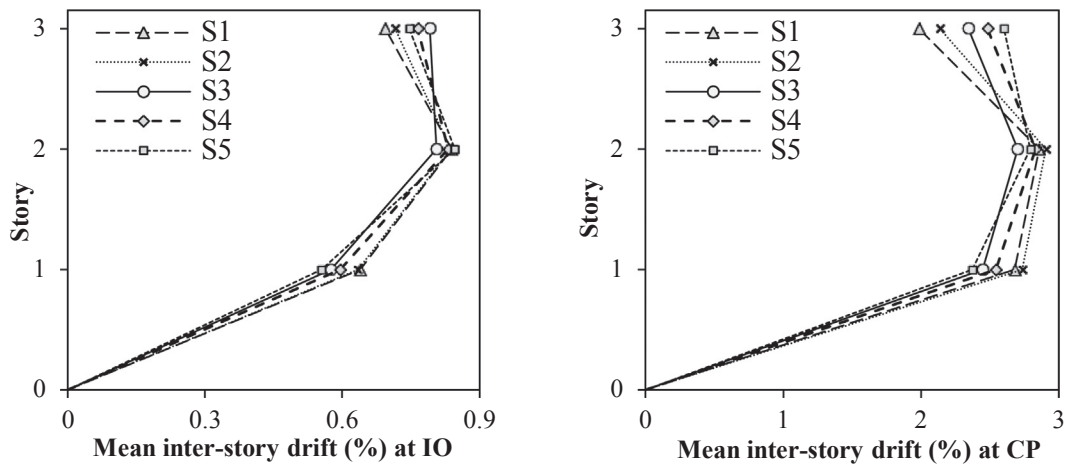


Fig. 7. Mean inter-story drifts of the 3-story optimal designs at IO and CP performance levels.

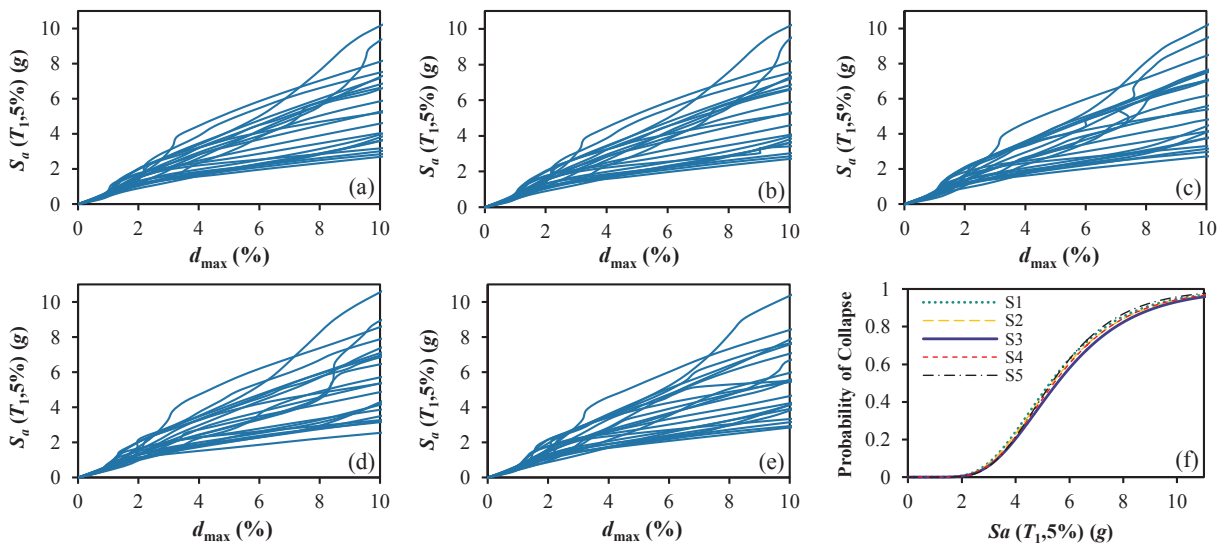


Fig. 8.  $d_{max}$ -based IDA curves for the 3-story optimal designs (a) S1, (b) S2, (c) S3, (d) S4, (e) S5 and (f) their collapse fragility curves.

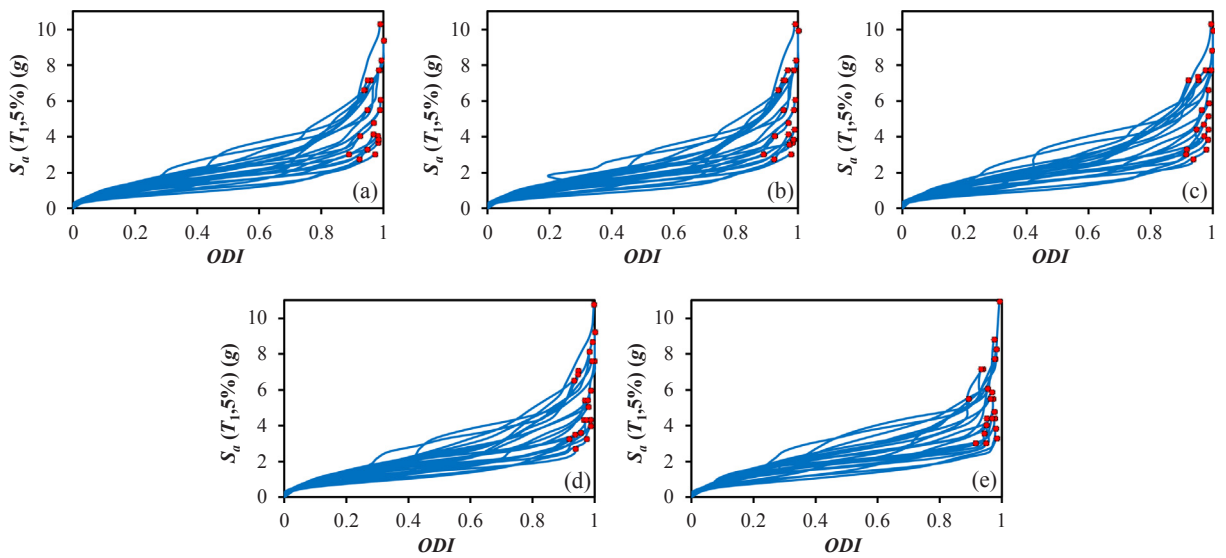


Fig. 9. ODI-based IDA curves for the 3-story optimal designs (a) S1, (b) S2, (c) S3, (d) S4, (e) S5.

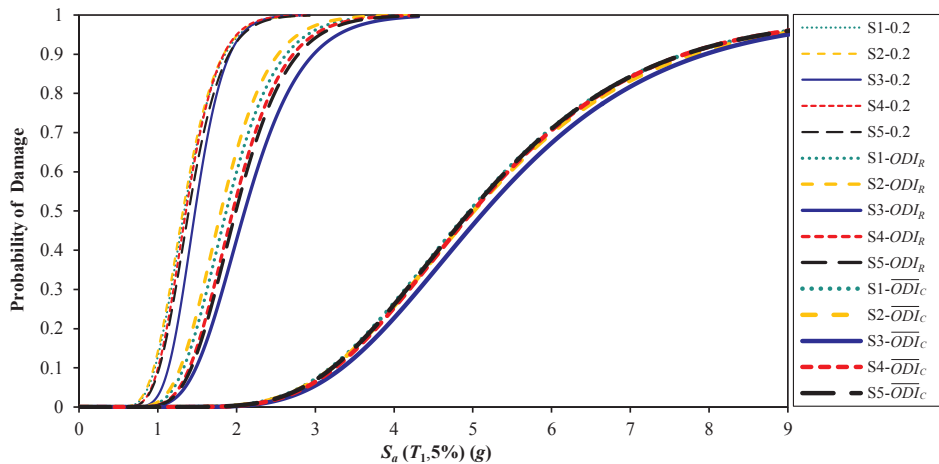


Fig. 10. ODI-based fragility curves for the 3-story optimal designs at different damage levels.

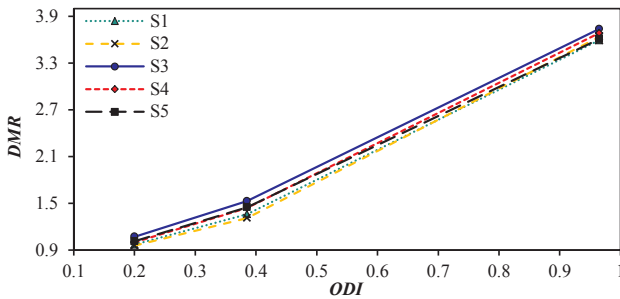


Fig. 11. DMR for the 3-story optimal designs at different damage levels.

Table 2, chosen from FEMA-P695, are considered and scaled to the 5%-damped acceleration response spectra of FE and MCE hazard levels presented in ASCE/SEI 7-10 [31] and seismic responses of SMFs are computed at IO and CP performance levels for the corresponding scaled records during the optimization process. In order to account for the stochastic nature of the optimization algorithm, 25 independent runs are performed and among the obtained optimal designs, 5 best solutions are taken into account.

In the second phase, incremental dynamic analyses are carried out using the records of Table 2 and  $d_{max}$ -based and ODI-based IDA curves are determined for all the obtained optimal designs. Afterward, the fragility curves are generated for different damage states and the values of ACMR and  $DMR_{ODI}$  are computed. In addition, the reparability border is determined for all the optimal designs and therefore the total costs of the structures,  $C_T$ , are calculated using Eqs. (9)–(14).

In the third phase, the optimal 3-, 6-, and 12-story SMFs are compared in terms of collapse safety, damage margin ratio at various levels of damage, total cost, and reparability and the best ones of low-, mid-, and high-rise SMFs are presented. Flowchart of the proposed methodology is depicted in Fig. 4.

Table 5  
Five best optimal solutions for 3-story SMF.

Optimal SMF	$C_0$ (kg)	ODI at CP level	$ODI_C$	$ODI_R$	$C_T$ (kg)	ACMR	DMR at ODI				$S_a$ 50% (g) from fragility curve based on			
							0.2	$ODI_R$	$ODI_C$	$d_{max}$	ODI			
S1	3075.66	0.41	0.963	0.385	7754.77	4.59	0.971	1.362	3.593	5.28	4.96			
S2	3084.75	0.44	0.967	0.387	8095.05	4.67	0.956	1.311	3.636	5.37	5.02			
S3	3104.59	0.38	0.968	0.387	7459.50	4.82	1.072	1.528	3.737	5.54	5.16			
S4	3123.84	0.42	0.969	0.388	7954.52	4.77	1.000	1.442	3.685	5.40	5.01			
S5	3218.36	0.39	0.959	0.384	7887.85	4.63	1.014	1.449	3.607	5.32	4.98			

Table 6  
Five best optimal solutions for 6-story SMF.

Design variables	Optimum performance-based solutions				
	S1	S2	S3	S4	S5
C1	W14 × 48	W14 × 48	W14 × 48	W14 × 43	W14 × 43
C2	W14 × 48	W14 × 48	W14 × 48	W14 × 43	W14 × 43
C3	W14 × 30	W14 × 30	W14 × 30	W14 × 43	W14 × 43
C4	W14 × 53	W14 × 53	W14 × 61	W14 × 53	W14 × 61
C5	W14 × 48	W14 × 53	W14 × 48	W14 × 53	W14 × 53
C6	W14 × 48	W14 × 48	W14 × 48	W14 × 53	W14 × 53
B1	W10 × 26	W10 × 26	W12 × 26	W10 × 26	W12 × 26
B2	W10 × 26	W12 × 26	W10 × 26	W12 × 26	W10 × 26
B3	W10 × 26	W10 × 26	W10 × 26	W10 × 26	W10 × 26
$C_0$ (kg)	8382.58	8479.55	8528.26	8616.14	8755.94
$CL_{IO}$ (%)	99.11	99.10	99.23	99.10	99.23
$CL_{CP}$ (%)	99.24	99.15	99.32	98.95	99.31

### 7. Numerical examples

In order to illustrate the efficiency of the proposed methodology, three numerical examples of 3-, 6-, and 12-story SMFs, shown in Fig. 5, are presented.

Yielding stress and modulus of elasticity for steel materials are  $f_y = 235$  MPa and  $E = 210$  GPa, respectively. The dead load of  $Q_D = 24.5166$  kN/m and live load of  $Q_L = 9.8067$  kN/m are applied to all beams. A rigid diaphragm is considered at floor levels due to the presence of slabs. The constitutive law is bilinear with pure strain hardening slope equal to 3% of the elastic modulus. The sections of beams and columns are selected from a data base of W-shaped sections listed in Table 3. In addition, OpenSees [32] platform has been used to model and perform the structural analyses. Force-based nonlinear beam-column element with distributed plasticity is employed and second-order P-Delta effects are included by using the P-Delta co-ordinate transformation object. The other required computer programs

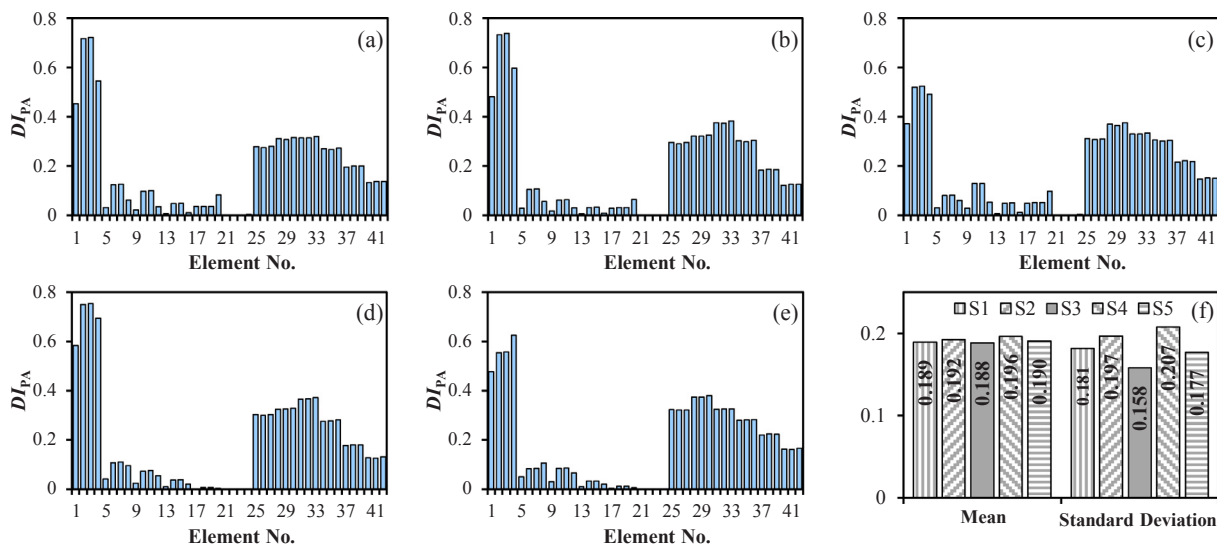


Fig. 12.  $D_{IPA}$  for members of 6-story (a) S1, (b) S2, (c) S3, (d) S4, (e) S5, and (f) their mean and standard deviation.

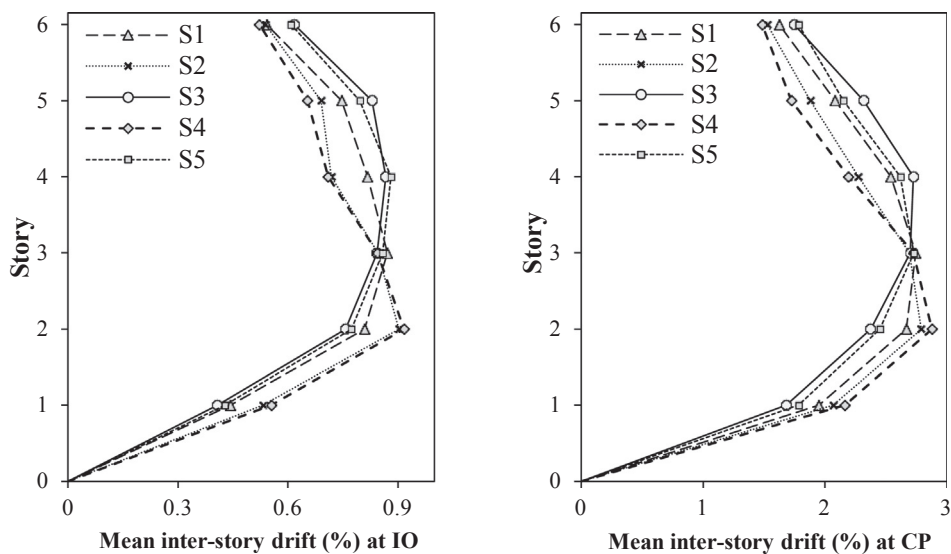


Fig. 13. Mean inter-story drifts of the 6-story optimal designs at IO and CP performance levels.

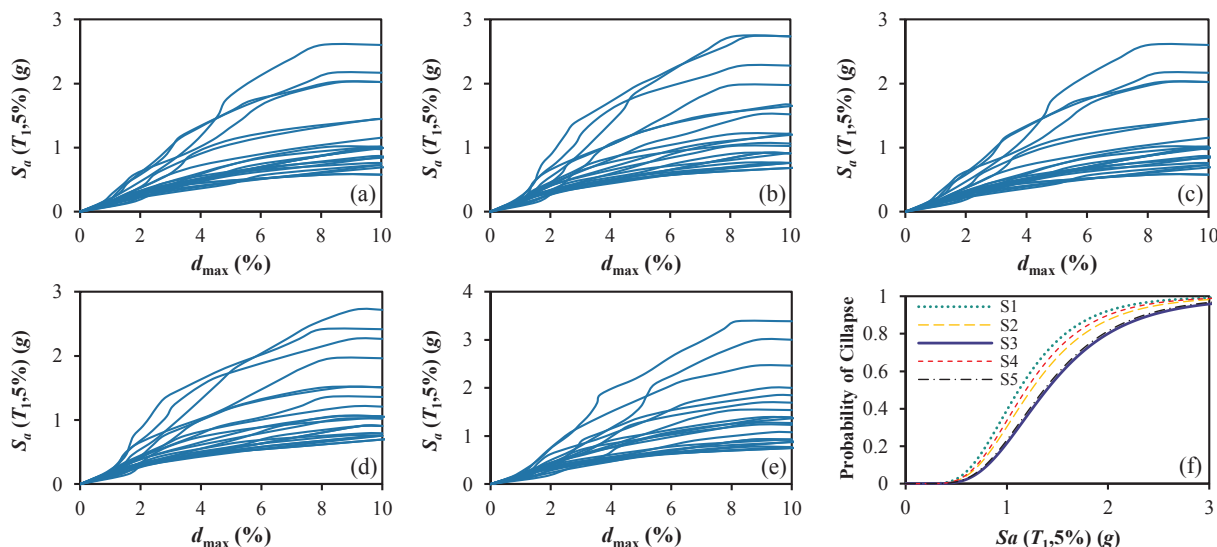


Fig. 14.  $d_{max}$ -based IDA curves for the 6-story optimal designs (a) S1, (b) S2, (c) S3, (d) S4, (e) S5 and (f) their collapse fragility curves.

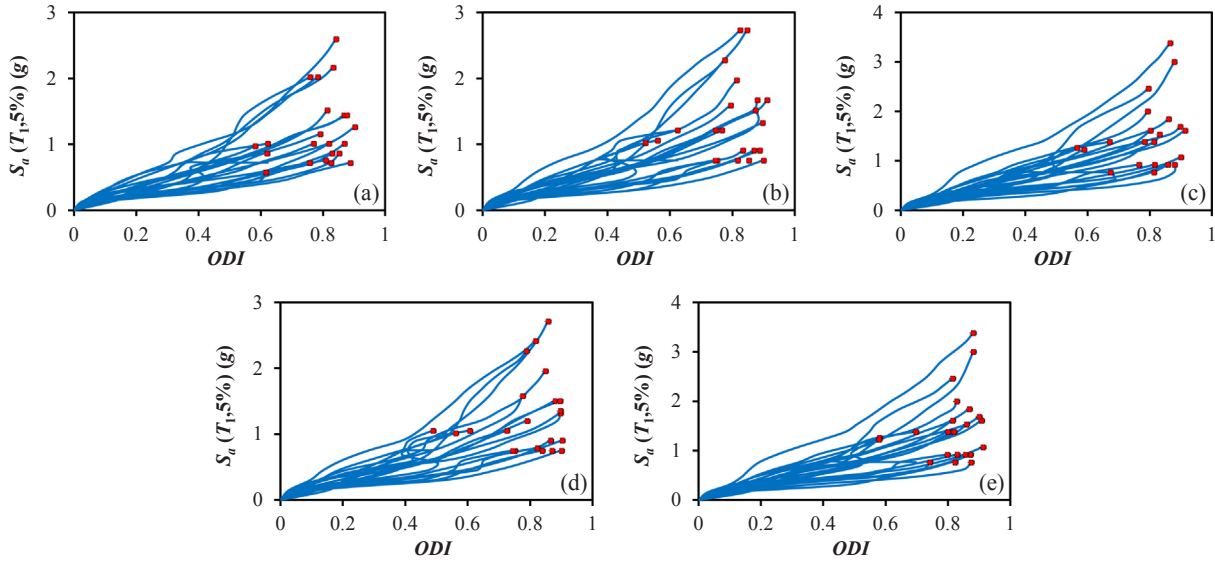


Fig. 15. ODI-based IDA curves for the 6-story optimal designs (a) S1, (b) S2, (c) S3, (d) S4, (e) S5.

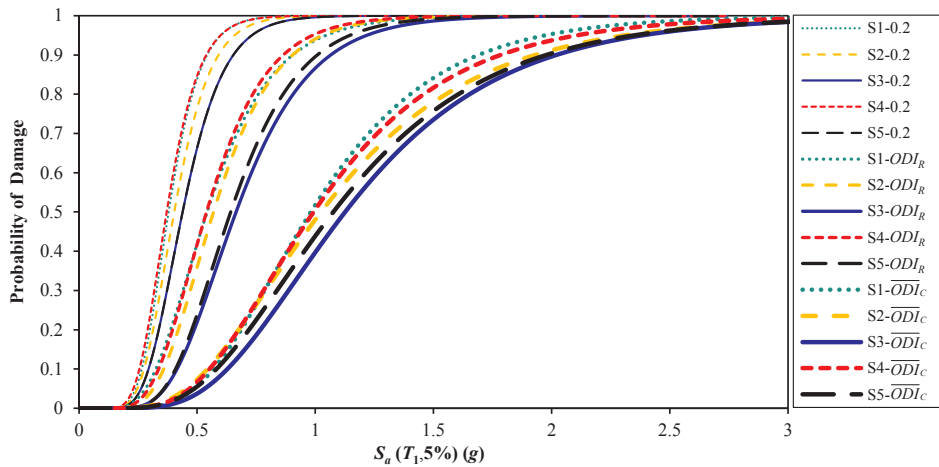


Fig. 16. ODI-based fragility curves for the 6-story optimal designs at different damage levels.

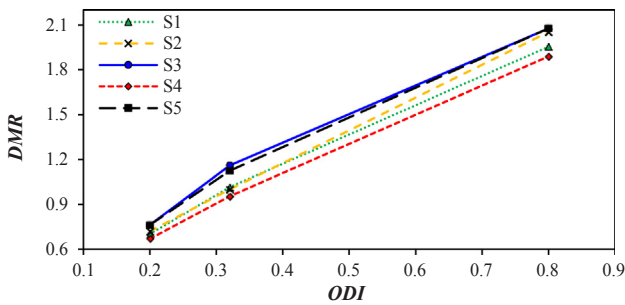


Fig. 17. DMR for the 6-story optimal designs at different damage levels.

to carry out optimization are coded in MATLAB [33].

### 7.1. 3-Story SMF

Five best optimal solutions obtained for 3-story SMF, denoted respectively by S1 to S5, are sorted in Table 4 by the increasing value of the initial cost  $C_0$  which the initial cost of S5 is 4.64% more than that of S1. In addition, confidence levels of the reported solutions at IO and CP performance levels demonstrate the feasibility of the solutions.

Fig. 6 (a) to (e) show  $DI_{PA}$  at CP performance level for members of

optimal solutions S1 to S5 and Fig. 6 (f) compares mean and standard deviation of  $DI_{PA}$  for these solutions. The results show that S3 has the least mean and standard deviation of  $DI_{PA}$  among all solutions. Additionally, the ODI values for the 3-story S1 to S5 solutions are 0.41, 0.44, 0.38, 0.42, and 0.39, respectively.

Mean inter-story drifts along with the height of the optimal 3-story SMFs at IO and CP performance levels are illustrated in Fig. 7. It can be seen that the least  $d_{max}$  at both IO and CP performance levels is related to the optimal solution of S3.

The results obtained from  $d_{max}$ -based incremental dynamic analyses of the 3-story optimal SMFs S1 to S5 subject to the set of 22 ground motions are illustrated in Fig. 8 (a) to (e), respectively. Moreover, the  $d_{max}$ -based collapse fragility curves of the SMFs are generated using the IDA curves and are shown in Fig. 8 (f). The ACMR for the S1 to S5 SMFs is 4.59, 4.67, 4.82, 4.77, and 4.63, respectively. As regards, based on FEMA P-695, the acceptable ACMR is equal to 1.56, the computed ACMRs indicate that all of these designs have considerable collapse safety and the highest ACMR belongs to S3.

ODI-based IDA curves are depicted in Fig. 9 for the 3-story optimal SMFs of S1 to S5. The mean value of ODI at collapse point,  $\overline{ODI}_C$ , for these optimal SMFs is 0.963, 0.967, 0.968, 0.969, and 0.959, respectively. Consequently, the reparability border,  $ODI_R$ , for the designs is 0.385, 0.387, 0.387, 0.388, and 0.384, respectively. The mean of  $ODI_R$

**Table 7**  
Five best optimal solutions for 6-story SMF.

Optimal SMF	C <sub>0</sub> (kg)	ODI at CP level	ODI <sub>C</sub>	ODI <sub>R</sub>	C <sub>T</sub> (kg)	ACMR	DMR at ODI		S <sub>a</sub> 50% (g) from fragility curve based on		
							0.2	ODI <sub>R</sub>	ODI <sub>C</sub>	d <sub>max</sub>	ODI
S1	8382.57	0.34	0.787	0.31	21516.55	2.48	0.70	1.01	1.95	1.12	1.06
S2	8479.55	0.38	0.795	0.32	22864.50	2.61	0.72	1.00	2.05	1.24	1.18
S3	8528.25	0.31	0.802	0.32	20330.74	2.87	0.77	1.16	2.09	1.38	1.19
S4	8616.14	0.40	0.796	0.32	24002.10	2.52	0.67	0.95	1.89	1.19	1.18
S5	8755.93	0.33	0.815	0.33	21264.40	2.84	0.74	1.12	2.07	1.36	1.09

**Table 8**  
Five best optimal solutions for 12-story SMF.

Design variables	Optimum performance-based solutions				
	S1	S2	S3	S4	S5
C1	W14 × 68	W14 × 61	W14 × 68	W14 × 53	W14 × 61
C2	W14 × 61	W14 × 48	W14 × 68	W14 × 53	W14 × 61
C3	W14 × 48	W14 × 48	W14 × 53	W14 × 53	W14 × 61
C4	W14 × 48	W14 × 48	W14 × 53	W14 × 53	W14 × 61
C5	W14 × 48	W14 × 43	W14 × 43	W14 × 48	W14 × 43
C6	W14 × 48	W14 × 43	W14 × 43	W14 × 48	W14 × 43
C7	W14 × 99	W14 × 82	W14 × 90	W14 × 74	W14 × 90
C8	W14 × 68	W14 × 82	W14 × 68	W14 × 74	W14 × 90
C9	W14 × 61	W14 × 74	W14 × 68	W14 × 74	W14 × 90
C10	W14 × 61	W14 × 74	W14 × 61	W14 × 74	W14 × 61
C11	W14 × 53	W14 × 61	W14 × 53	W14 × 61	W14 × 53
C12	W14 × 53	W14 × 61	W14 × 48	W14 × 61	W14 × 53
C13	W14 × 109	W14 × 109	W14 × 109	W14 × 109	W14 × 109
C14	W14 × 99	W14 × 82	W14 × 109	W14 × 82	W14 × 74
C15	W14 × 74	W14 × 68	W14 × 68	W14 × 68	W14 × 74
C16	W14 × 74	W14 × 61	W14 × 68	W14 × 68	W14 × 74
C17	W14 × 53	W14 × 53	W14 × 53	W14 × 68	W14 × 61
C18	W14 × 48	W14 × 48	W14 × 53	W14 × 61	W14 × 48
B1	W12 × 26	W12 × 26	W12 × 30	W12 × 26	W12 × 26
B2	W12 × 26	W12 × 26	W12 × 26	W12 × 26	W12 × 26
B3	W12 × 26	W12 × 30	W12 × 30	W12 × 26	W12 × 35
B4	W12 × 26	W12 × 30	W12 × 26	W12 × 35	W12 × 26
B5	W12 × 26	W12 × 26	W12 × 26	W12 × 26	W12 × 26
B6	W10 × 26	W10 × 26	W10 × 26	W12 × 26	W10 × 26
C <sub>0</sub> (kg)	26160.34	26440.32	26652.89	26884.21	27456.91
CL <sub>IO</sub> (%)	0.9986	0.9978	0.9986	0.9957	0.9986
CL <sub>CP</sub> (%)	0.9889	0.9889	0.9933	0.9889	0.9932

values for all the 3-story optimal designs is equal to 0.386. Furthermore, the total cost (C<sub>T</sub>) of SMFs S1 to S5 computed based on the ODI at CP performance level and ODI<sub>R</sub> are 7754.77, 8095.05, 7459.50, 7954.52, and 7887.85 kg, respectively.

In addition, ODI-based fragility curves and DMRs for different damage levels (ODI = 0.2, ODI<sub>R</sub>, and ODI<sub>C</sub>) are respectively shown in Figs. 10 and 11 for the 3-story S1 to S5 SMFs. The comparison of DMRs in Fig. 11 indicates that S3 SMF has the best DMR in all damage levels.

All of the obtained results in this example are summarized in Table 5. It is clear that S3 is the best design in terms of total cost and its C<sub>T</sub> is 3.81%, 7.85%, 6.22%, and 5.43% less than that of S1, S2, S4, and S5, respectively. Comparison of ODIs at CP Level with ODI<sub>R</sub> reveals that only S3 is repairable and the other designs are unreparable. Moreover, it can be observed that, as the best design, S3 SMF has the highest ACMR and DMR values at different damage levels in comparison with other optimal solutions. ACMR of S3 is 5.01%, 3.21%, 1.05%, and 4.10% more than that of S1, S2, S4, and S5, respectively. In addition, ODI<sub>R</sub> of S3 is 12.19%, 16.55%, 5.96%, and 5.45% more than that of S1, S2, S4, and S5, respectively. Furthermore, the median collapse S<sub>a</sub> evaluated from the d<sub>max</sub> and ODI-based collapse fragility curves are compared in Table 5. It can be observed that S<sub>a</sub> 50% values obtained from ODI-based collapse fragility curves are less than those of d<sub>max</sub>-based collapse fragility curves.

7.2. 6-Story SMF

Table 6 reports five best optimal solutions for 6-story SMF. The difference between maximum and minimum of C<sub>0</sub> is 4.26% only. The feasibility of the optimal designs is demonstrated based on the values of CL at IO and CP performance levels.

For the members of 6-story optimal solutions S1 to S5, DI<sub>PA</sub> at CP

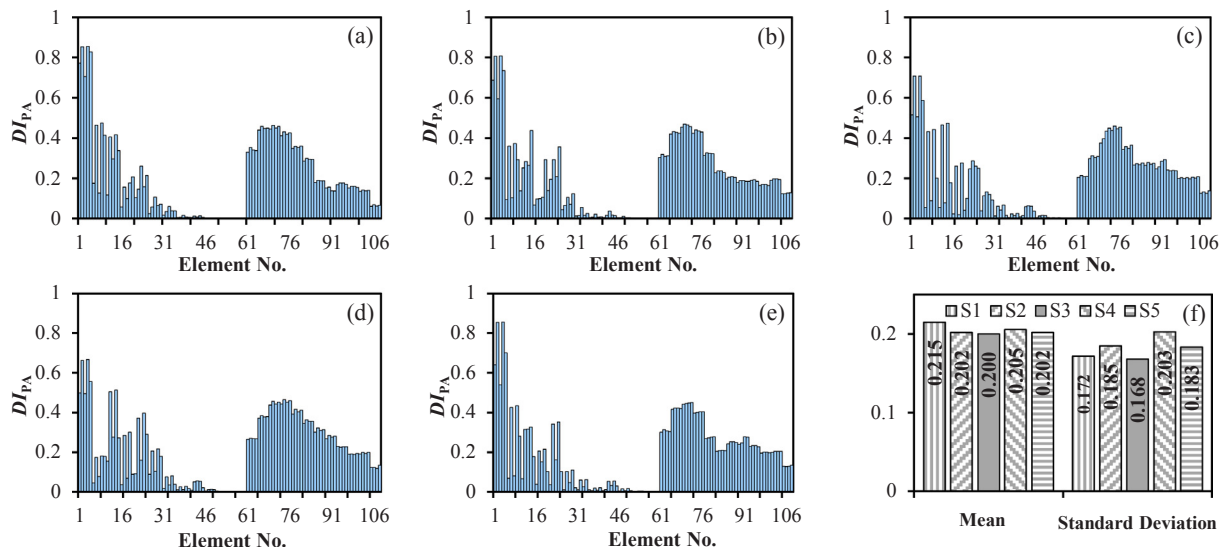


Fig. 18. DI<sub>PA</sub> for members of 12-story (a) S1, (b) S2, (c) S3, (d) S4, (e) S5, and (f) their mean and standard deviation.

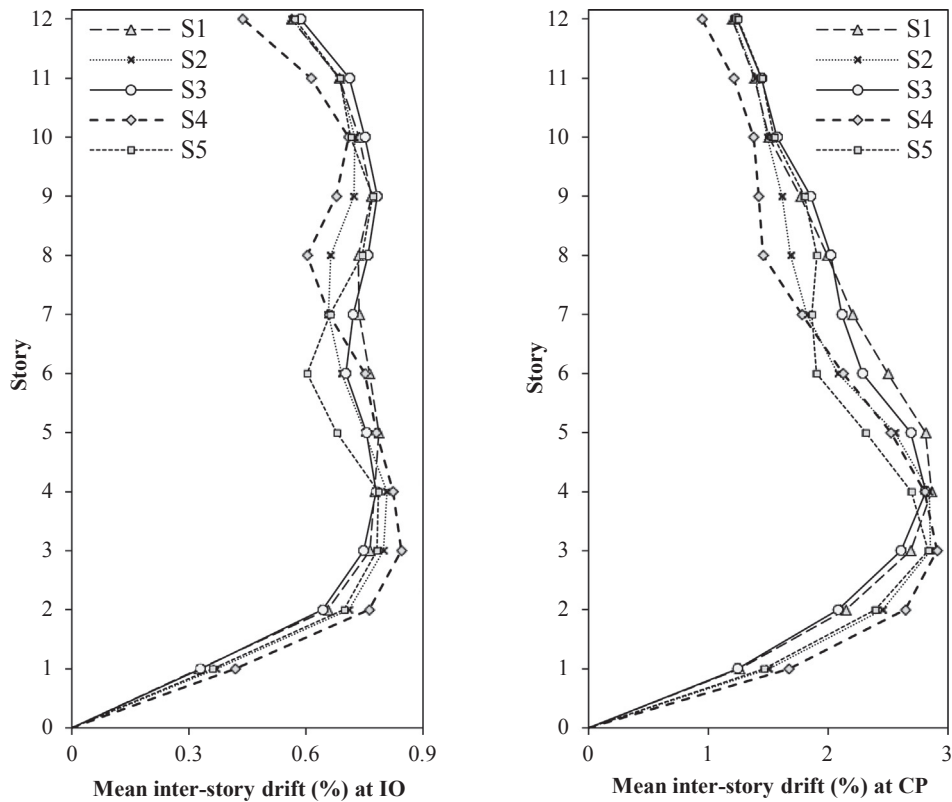


Fig. 19. Mean inter-story drifts of the 12-story optimal designs at IO and CP performance levels.

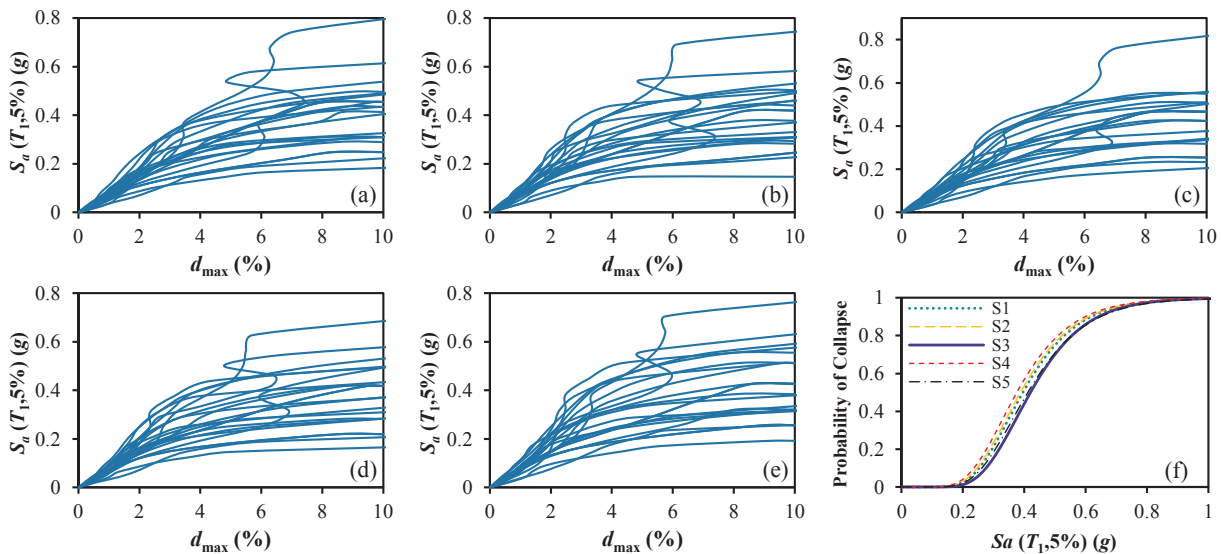


Fig. 20.  $d_{max}$ -based IDA curves for the 12-story optimal designs (a) S1, (b) S2, (c) S3, (d) S4, (e) S5 and (f) their collapse fragility curves.

performance level are depicted in Fig. 12 (a) to (e), respectively and the mean and standard deviation of  $DI_{PA}$  for the SMFs are compared in Fig. 12 (f). The results show that S3 has the least mean and standard deviation of  $DI_{PA}$  among all solutions. Furthermore, for the 6-story S1 to S5 SMFs, the values of  $ODI$  at CP performance level are 0.34, 0.38, 0.31, 0.40, and 0.33, respectively.

Fig. 13 compares the mean inter-story drift profile of the optimal 6-story SMFs at IO and CP performance levels. It can be seen that the drift profiles of S3 and S5 are very close to each other and the least  $d_{max}$  at both IO and CP performance levels belongs to the optimal solution of S3.

The  $d_{max}$ -based IDA curves of the 6-story optimal S1 to S5 SMFs are

shown in Fig. 14 (a) to (e), respectively. Moreover, the  $d_{max}$ -based collapse fragility curves of the optimal SMFs are generated using the IDA curves and are shown in Fig. 14 (f). The  $ACMR$ s for the 6-story optimal S1 to S5 SMFs are 2.48, 2.61, 2.87, 2.52, and 2.84, respectively which all are greater than the acceptable  $ACMR$  of 1.56 [15] and this means that all of the designs are of considerable collapse safety and S3 has the highest  $ACMR$ .

Fig. 15 illustrates  $ODI$ -based IDA curves of the 6-story S1 to S5 SMFs. The mean value of  $ODI$  at collapse point,  $\overline{ODI}_C$ , for the 6-story S1 to S5 SMFs is 0.787, 0.795, 0.802, 0.796, and 0.815, respectively. Consequently, the reparability border,  $ODI_R$ , for these designs is 0.315, 0.318, 0.321, 0.318, and 0.326, respectively. The mean of  $ODI_R$  values

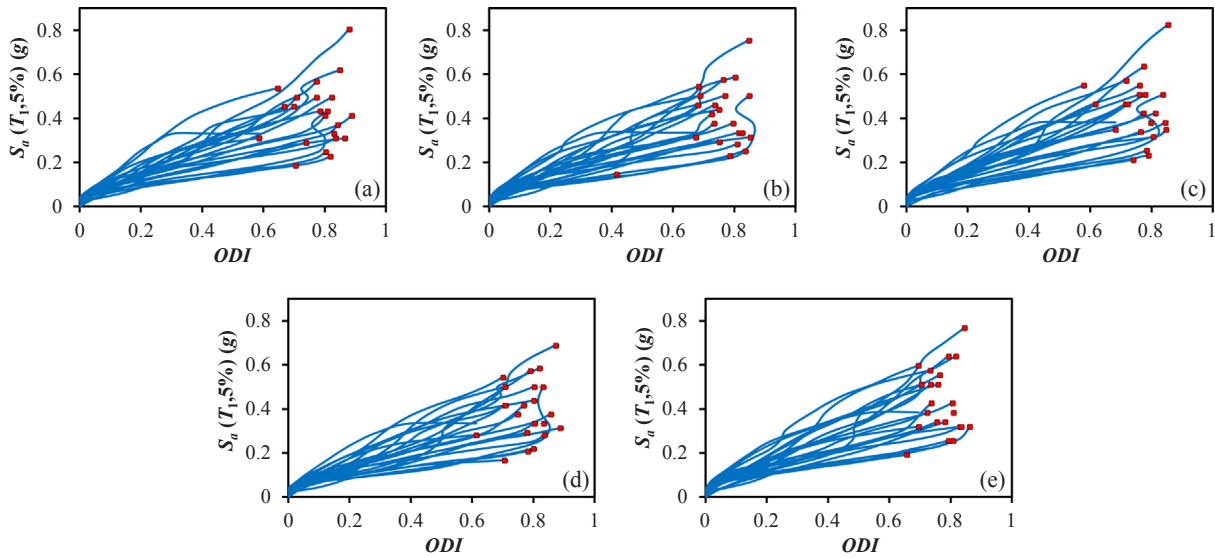


Fig. 21. ODI-based IDA curves for the 12-story optimal designs (a) S1, (b) S2, (c) S3, (d) S4, (e) S5.

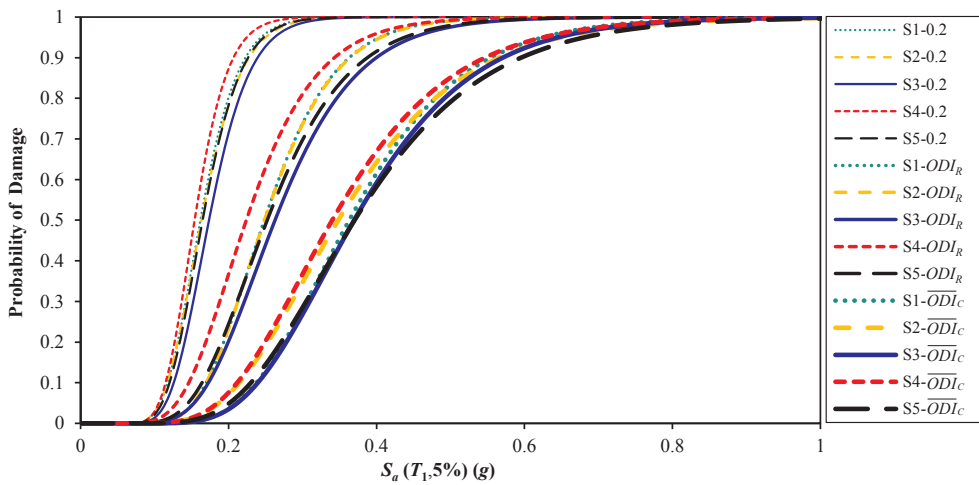


Fig. 22. ODI-based fragility curves for the 12-story optimal designs at different damage levels.

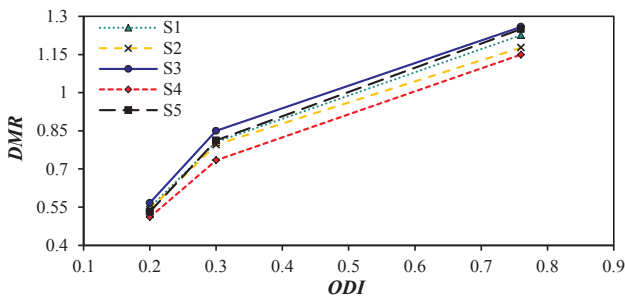


Fig. 23. DMR for the 12-story optimal designs at different damage levels.

for all the 6-story optimal designs is equal to 0.320. Furthermore,  $C_T$  of SMFs S1 to S5 computed based on the ODI at CP performance level and  $ODI_R$  are 21516.55, 22864.50, 20330.74, 24002.10, and 21264.40 kg, respectively.

Figs. 16 and 17 show ODI-based fragility curves and DMRs at different damage levels respectively for the 6-story S1 to S5 SMFs. The comparison of DMRs in Fig. 17 indicates that S3 SMF has the best DMR in all the damage levels.

Table 7 summarizes the results of this example for the SMFs of S1 to S5. It is clear that S3 is the best design in terms of total cost and its  $C_T$  is

5.51%, 11.08%, 15.29%, and 4.39% less than that of S1, S2, S4, and S5, respectively. Comparison of ODI at CP Level with  $ODI_R$  of the optimal designs indicates that only S3 and S5 are repairable and the other ones are unreparable. Moreover, it can be observed that, the highest ACMR and DMR values at different damage levels belong to SMF S3. ACMR of S3 is 15.73%, 9.96%, 13.89%, and 1.05% more than that of S1, S2, S4, and S5, respectively. In addition,  $ODI_R$  of all designs is very close to each other. Table 7 compares the median collapse  $S_a$  evaluated from the  $d_{max}$  and ODI-based collapse fragility curves indicating that  $S_a$  50% values obtained from ODI-based collapse fragility curves are less than those of  $d_{max}$ -based collapse fragility curves.

### 7.3. 12-Story SMF

For the 12-story SMF, five best optimal solutions of S1 to S5 are sorted in Table 8 indicating that  $C_0$  of S5 is 4.72% more than that of S1. Additionally, the values of CL at IO and CP performance levels demonstrate that the optimal designs are feasible.

$DI_{PA}$  at CP performance level for members of 12-story optimal designs S1 to S5 and their corresponding mean and standard deviation of  $DI_{PA}$  are shown in Fig. 18 implying that the S3 solution has the least mean and standard deviation of local damages. The overall damage index is determined for these solutions and the results reveal that the

**Table 9**  
Five best optimal solutions for 12-story SMF.

Optimal SMF	$C_0$ (kg)	ODI at CP level	$\bar{ODI}_C$	$ODI_R$	$C_T$ (kg)	ACMR	DMR at ODI			$S_a$ 50% (g) from fragility curve based on	
							0.2	$ODI_R$	$\bar{ODI}_C$	$d_{max}$	ODI
S1	26160.34	0.33	0.779	0.31	65943.35	1.66	0.55	0.81	1.23	0.39	0.38
S2	26440.32	0.33	0.754	0.30	67989.39	1.61	0.54	0.79	1.18	0.39	0.37
S3	26652.89	0.30	0.762	0.30	64728.45	1.72	0.57	0.85	1.26	0.42	0.40
S4	26884.21	0.37	0.779	0.31	72723.65	1.56	0.51	0.73	1.15	0.37	0.36
S5	27456.91	0.33	0.770	0.31	69211.66	1.68	0.53	0.81	1.25	0.41	0.40

values of  $ODI$  at CP performance level are 0.33, 0.33, 0.31, 0.37, and 0.33, respectively.

For the 12-story optimal SMFs, the mean inter-story drift profiles at IO and CP performance levels are compared in Fig. 19 indicating that in the inter-story drift profiles of S1 to S5 the least  $d_{max}$  at both IO and CP performance levels is observed in that of the S3 solution.

Fig. 20 (a) to (e) depict the  $d_{max}$ -based IDA curves for the 12-story S1 to S5 SMFs, respectively and Fig. 20 (f) shows the  $d_{max}$ -based collapse fragility curves of these optimal structures. For the 12-story S1 to S5 SMFs, the  $ACMR$  values are 1.66, 1.62, 1.72, 1.57, and 1.68, respectively which all are greater than the acceptable  $ACMR$  of 1.56 [15] and this means that the collapse safety of the optimal 12-story SMFs is acceptable and the  $ACMR$  of S3 is the maximum among all the designs.

For the 12-story S1 to S5 SMFs, the  $ODI$ -based IDA curves are depicted in Fig. 21. For the designs of S1 to S5,  $\bar{ODI}_C$  values are 0.779, 0.754, 0.762, 0.779, and 0.770, respectively. As a result, the values of  $ODI_R$  for these designs are 0.31, 0.30, 0.30, 0.31, and 0.31, respectively. The mean of  $ODI_R$  values for all the 12-story optimal designs is equal to 0.306. In addition,  $C_T$  of S1 to S5 SMFs computed based on the  $ODI$  at CP performance level and  $ODI_R$  are 65943.35, 67989.39, 64728.45, 72723.65, and 69211.66 kg, respectively.

The  $ODI$ -based fragility curves of the 12-story optimal designs and their  $DMR$ s at different damage levels are shown in Figs. 22 and 23, respectively. It can be seen from Fig. 23 that the best  $DMR$  at all the damage levels belongs to S3 SMF.

In the Table 9 a summary of the obtained results for the 12-story SMF is reported. The comparison of  $C_T$  of the optimal solutions indicate that the best design is S3 and its  $C_T$  is 1.84%, 4.80%, 10.99%, and 6.48% less than that of S1, S2, S4, and S5, respectively. On the other hand, S3 is the only design that its  $ODI$  at CP Level is less than its corresponding  $ODI_R$  and therefore it is repairable while the other ones are unreparable. The results also show that the highest  $ACMR$  and  $DMR$  values at different damage levels belong to SMF S3.  $ACMR$  of S3 is 3.61%, 6.83%, 10.26%, and 2.38% more than that of S1, S2, S4, and S5, respectively. In addition,  $ODI_R$  of all designs is almost identical. Comparison of the median collapse  $S_a$  evaluated from the  $d_{max}$  and  $ODI$ -based collapse fragility curves in Table 9 reveals that  $S_a$  50% values obtained from  $ODI$ -based collapse fragility curves are less than their corresponding values obtained from  $d_{max}$ -based collapse fragility curves.

## 8. Conclusions

The main aim of the present study is to propose a methodology for assessing seismic collapse-resistant capacity and repairability of optimally designed SMFs. In order to achieve this purpose, initial cost ( $C_0$ ) of SMFs is optimized in the framework of PBD based on the requirements of FEMA-350 using the ECBO-II metaheuristic algorithm. The local damages distribution and the overall damage index of the optimal SMFs are determined using the Park-Ang damage index. Afterward, the IDA is implemented for the optimally designed SMFs and their fragility curves are generated to compute their  $ACMR$  values based on the methodology of FEMA-P695. Finally, the  $ODI$ -based fragility curves are generated at different damage levels to compute the newly proposed

$DMR$  indicator for the optimally designed SMFs. Three design examples including 3-, 6-, and 12-story SMFs are presented to demonstrate the efficiency of the proposed methodology. As regards such an optimization process is of a stochastic nature, twenty-five independent optimization runs are carried out for each example and among the solutions, five best ones are selected. The main concluding remarks of this study can be summarized as follows:

1. In all examples of 3-, 6-, and 12-story SMFs, it is observed that the best solutions, having the least  $C_T$ , have the best seismic damages distribution with the least mean and standard deviation of  $DI_{PA}$  and consequently the least  $ODI$  among all solutions.
2. The least  $d_{max}$  in the inter-story drift profiles of different 3-, 6-, and 12-story optimal SMFs occurs at both IO and CP performance levels in the case of solutions having the least  $C_T$ .
3. The results show that in all examples, the highest  $ACMR$  belongs to the optimal designs with the least total cost  $C_T$ . For these best 3-, 6-, and 12-story SMFs, the  $ACMR$  values are 4.82, 2.87, and 1.72, respectively.
4. In 3- and 12-story examples, among the obtained optimal solutions, only the best one with the least  $C_T$  and in 6-story example two first best solutions, in terms of  $C_T$ , satisfy the repairability condition proposed in this study and the other ones are unreparable. Furthermore, for each example, the superiority of the best design over the other ones is demonstrated in terms of  $DMR$  at different damage levels.
5. In all examples, the comparison of the median collapse  $S_a$  evaluated from the  $d_{max}$  and  $ODI$ -based collapse fragility curves reveals that  $S_a$  50% obtained from  $ODI$ -based collapse fragility curves represents a higher collapse risk.
6. Based on the findings of the present study, it can be asserted that the collapse of different 3-, 6-, and 12-story SMFs occurs in a damage level in which the overall damage index is less than unity and this indicates that the repairability border of  $ODI = 0.4$  should be enhanced. In this work, the repairability border for the 3-, 6-, and 12-story optimal SMFs is proposed to be 0.39, 0.32, and 0.30, respectively.

It can be concluded that optimization of total cost of SMFs will result in a design with considerable collapse safety, appropriate damage margin ratio and uniform damage distribution in which an appropriate trade-off between total cost and seismic safety can be achieved.

Finally, it should be noted that all the numerical examples are based on the optimized SMF structures. For the real structure which is not optimized, the conclusions such as the repairability border of  $ODI$  could be different.

## Appendix A. Supplementary material

Supplementary data to this article can be found online at <https://doi.org/10.1016/j.engstruct.2018.10.075>.

## References

- [1] Choi SW, Park HS. Multi-objective seismic design method for ensuring beam hinging mechanism in steel frames. *J Constr Steel Res* 2012;74:17–25.
- [2] Saadat S, Camp CV, Pezeshk S. Seismic performance-based design optimization considering direct economic loss and direct social loss. *Eng Struct* 2014;76:193–201.
- [3] Gholizadeh S. Performance-based optimum seismic design of steel structures by a modified firefly algorithm and a new neural network. *Adv Eng Softw* 2015;81:50–65.
- [4] Gholizadeh S, Poorhoseini H. Seismic layout optimization of steel braced frames by an improved dolphin echolocation algorithm. *Struct Multidisc Optim* 2016;54:1011–29.
- [5] Xu J, Spencer BF, Lu X. Performance-based optimization of nonlinear structures subject to stochastic dynamic loading. *Eng Struct* 2017;134:334–45.
- [6] Gholizadeh S, Baghchevan A. Multi-objective seismic design optimization of steel frames by a chaotic meta-heuristic algorithm. *Eng Comput* 2017;33:1045–60.
- [7] Shafei B, Zareian F, Lignos DG. A simplified method for collapse capacity assessment of moment-resisting frame and shear wall structural systems. *Eng Struct* 2011;33:1107–16.
- [8] Hardyniec A, Charney F. A new efficient method for determining the collapse margin ratio using parallel computing. *Comput Struct* 2015;148:15–25.
- [9] Vamvatsikos D, Cornell CA. Incremental dynamic analysis. *Earthquake Eng Struct Dynam* 2002;31:491–514.
- [10] Asgarian B, Ordoubadi B. Effects of structural uncertainties on seismic performance of steel moment resisting frames. *J Constr Steel Res* 2016;120:132–42.
- [11] Cha YJ, Bai JW. Seismic fragility estimates of a moment-resisting frame building controlled by MR dampers using performance-based design. *Eng Struct* 2016;116:192–202.
- [12] Gholizadeh S, Milany A. Optimal performance-based design of steel frames using advanced metaheuristics. *Asian J Civil Eng* 2016;17:607–23.
- [13] Kaveh A, Ilchi Ghazaan M. Enhanced colliding bodies optimization for design problems with continuous and discrete variables. *Adv Eng Softw* 2014;77:66–75.
- [14] FEMA-350. Recommended seismic design criteria for new steel moment-frame buildings. Washington (DC): Federal Emergency Management Agency; 2000.
- [15] FEMA-P695. Quantification of building seismic performance factors. Washington (DC): Federal Emergency Management Agency; 2009.
- [16] Park YJ, Ang AH-S. Mechanistic seismic damage model for reinforced concrete. *ASCE J Struct Eng* 1985;111:722–39.
- [17] AISC 360-16. Specification for structural steel buildings. Chicago: American Institute of Steel Construction; 2016.
- [18] AISC 341-16. Seismic provisions for structural steel buildings. Chicago: American Institute of Steel Construction; 2016.
- [19] Gholizadeh S, Mohammadi M. Reliability-based seismic optimization of steel frames by metaheuristics and neural networks. *ASCE-ASME J Risk Uncertainty Eng Syst Part A: Civ Eng* 2017;3:1–11.
- [20] Ghosh S, Datta D, Katakhdond AA. Estimation of the Park-Ang damage index for planar multi-storey frames using equivalent single-degree systems. *Eng Struct* 2011;33:2509–24.
- [21] Kazantzi AK, Vamvatsikos D. The hysteretic energy as a performance measure in analytical studies. *Earthq Spectra* 2018;34:719–39.
- [22] Priestley MJN. Myths and fallacies in earthquake engineering-conflicts between design and reality. *Bull NZ Natl Soc Earthquake Eng* 1993;26:329–41.
- [23] Park YJ, Ang AH, Wen YK. Damage-limiting aseismic design of buildings. *Earthq Spectra* 1987;3:1–26.
- [24] Moller O, Foschi RO, Quiroz L, Rubinstein M. Structural optimization for performance-based design in earthquake engineering: applications of neural networks. *Struct Safety* 2009;31:490–9.
- [25] HAZUS-MH MR1. Multi-hazard Loss Estimation Methodology Earthquake Model. Washington (DC): FEMA-National Institute of Building Sciences; 2003.
- [26] Kang YJ, Wen YK. Minimum life-cycle cost structural design against natural hazards. Tech. Rep. SRS 629. University of Illinois at Urbana-Champaign; 2000.
- [27] Rajeev P, Wijesundara KK. Energy-based damage index for concentrically braced steel structure using continuous wavelet transform. *J Constr Steel Res* 2014;103:241–50.
- [28] Bojórquez E, Reyes-Salazar A, Terán-Gilmore A, Ruiz SE. Energy-based damage index for steel structures. *Steel Compos Struct* 2010;10:343–60.
- [29] Cao H, Friswell MI. The effect of energy concentration of earthquake ground motions on the nonlinear response of RC structures. *Soil Dyn Earthq Eng* 2009;29:292–9.
- [30] ATC-13. Earthquake Damage Evaluation Data for California. Washington (DC): Applied Technology Council; 1985.
- [31] ASCE/SEI 7-10. Minimum Design Loads and Associated Criteria for Buildings and other Structures. Washington (DC): American Society of Civil Engineers; 2010.
- [32] OpenSees version 2.4.0 [Computer software]. PEER, Berkeley, CA.
- [33] MATLAB. The language of technical computing. Math Works Inc.; 2016.